Open Access Full Text Article

ORIGINAL RESEARCH

Real-time monitoring of cisplatin cytotoxicity on three-dimensional spheroid tumor cells

NamHuk Baek[1,*]
Ok Won Seo[1,*]
Jaehwa Lee[1]
John Hulme[2]
Seong Soo A An[2]

[1]Department of Research and Development, NanoEntek Inc., Seoul, [2]Department of BioNano Technology, Gachon University, Gyeonggi-do, Korea

*These authors contributed equally to this work

Video abstract

Correspondence: Seong Soo A An
Department of BioNano Technology, Gachon Medical Research Institute, Gachon University, 1342 Sungnam Daero, Sungnamsi 461-701, Korea
Tel +82 31 750 8755
Fax +82 31 750 8755
Email seongaan@gachon.ac.kr

Abstract: Three-dimensional (3D) cell cultivation is a powerful technique for monitoring and understanding diverse cellular mechanisms in developmental cancer and neuronal biology, tissue engineering, and drug development. 3D systems could relate better to in vivo models than two-dimensional (2D) cultures. Several factors, such as cell type, survival rate, proliferation rate, and gene and protein expression patterns, determine whether a particular cell line can be adapted to a 3D system. The 3D system may overcome some of the limitations of 2D cultures in terms of cell–cell communication and cell networks, which are essential for understanding differentiation, structural organization, shape, and extended connections with other cells or organs. Here, the effect of the anticancer drug cisplatin, also known as cis-diamminedichloroplatinum (II) or CDDP, on adenosine triphosphate (ATP) generation was investigated using 3D spheroid-forming cells and real-time monitoring for 7 days. First, 12 cell lines were screened for their ability to form 3D spheroids: prostate (DU145), testis (F9), embryonic fibroblast (NIH-3T3), muscle (C2C12), embryonic kidney (293T), neuroblastoma (SH-SY5Y), adenocarcinomic alveolar basal epithelial cell (A549), cervical cancer (HeLa), HeLa contaminant (HEp2), pituitary epithelial-like cell (GH3), embryonic cell (PA317), and osteosarcoma (U-2OS) cells. Of these, eight cell lines were selected: NIH-3T3, C2C12, 293T, SH-SY5Y, A549, HeLa, PA317, and U-2OS; and five underwent real-time monitoring of CDDP cytotoxicity: HeLa, A549, 293T, SH-SY5Y, and U-2OS. ATP generation was blocked 1 day after addition of 50 µM CDDP, but cytotoxicity in HeLa, A549, SH-SY5Y, and U-2OS cells could be visualized only 4 days after treatment. In 293T cells, CDDP failed to kill entirely the culture and ATP generation was only partially blocked after 1 day. This suggests potential CDDP resistance of 293T cells or metabolic clearance of the drug. Real-time monitoring and ATP measurements directly confirmed the cytotoxicity of CDDP, indicating that CDDP may interfere with mitochondrial activity.

Keywords: cisplatin, real-time monitoring, cytotoxicity, 3D spheroids, ATP productions

Introduction

Cells are usually grown as two-dimensional (2D) cultures, which are reliable and convenient for the majority of developmental biology, tissue engineering, tissue formation, disease mechanism, drug development, and especially large-scale therapeutic protein production studies.[1] The recent development of three-dimensional (3D) culture systems has offered a model closer to in vivo conditions and promised to advance our understanding of cell survival, proliferation, differentiation, and gene and protein expression.[2] Morphological and other properties exhibited by cells in 3D cultures may be better suited for studies of structural organization, cell–cell communication, cell–extracellular matrix interaction, drug sensitivity, cell death, cancer cell survival, and neighboring cell networks.[3] The ensuing results could have a profound influence on studies in cancer biology, drug toxicity tests, stem cell applications, and

2155

tissue engineering. For example, 3D culture systems could be applied to the study of vasculogenic mimicry, which is currently severely limited in 2D cultures.[4] In terms of drug testing and cancer research, growth rates, shapes, and responses are likely different in 3D cultures, compared to 2D cultures, and bear greater resemblance to in vivo models of gene expressions.[5,6]

According to Mikhail et al, 3D cultures could represent an intermediate step between 2D cultures and in vivo models and would be especially useful for monitoring initial cellular responses, such as cytotoxicity and drug resistance. Results may help improve planning of animal studies.[5] The first step in developing a 3D culture system would be to determine the ability of cell lines to form 3D spheroids. At present, more than 380 cell lines have been tested for their potential to form and maintain 3D spheroids, among these: SF268, SH-SY5Y, U-2OS, MDA-MB-231, MCF-7, HCT116, and an additional 40 cell lines.[7] In another study, A2780, OV2008, SKOV-3, plus 32 other cell lines were tested and a dozen were confirmed to form 3D spheroids.[8] Each cell line produced spheroids of varying shape and size, which could be classified as tight, compact, or loose aggregates. The following cell lines were unable to form spheroids: 1847, A2780, CaOV3, COV644, EFO27, ES-2, FUOV1, HEY, IGROV1, JAMA-2, LK2, OAWA42, OC316, OV2008, OVCAR429, OV-MZ-15, PXN94, SKOV-3, TOV112D, and UWB1.289.[8]

Cis-diamminedichloridoplatinum (II) (known as cisplatin or CDDP) is a well-known alkylating agent with anticancer properties. By binding to guanine nucleotide bases, it blocks DNA replication causing DNA damage and cell cycle arrests.[9] CDDP was reported to be effective against lung, ovarian, and prostate cancers.[10] However, several cell lines have shown resistance to CDDP[11,12] and several side effects have been documented, such as nephrotoxicity, infertility, ototoxicity, and neurotoxicity, which would limit its long-term usage.[13] Previous studies reported that cancer cell lines Hep3B, HepJ5, ES-2, SKOV-3, OVCAR-3, and MCF-7 suffered a significant loss in cell viability upon CDDP treatment in 2D cultures.[9,14–16] Contrary to 2D cultures, when uterus/endometrium cell lines, such as Ishikawa, RL95-2, KLE, and the colon carcinoma cell line HCT116 were used to assess the effect of CDDP, no significant loss of viability was observed in 3D systems.[17,18] Instead, cell viability was greatly reduced upon CDDP treatment of 3D bone osteosarcoma cell lines (Saos-2, HOS).[19] Therefore, variations to drug sensitivity and tolerance could be better understood with a 3D cell culture system.

In this study, the effect of the anticancer drug CDDP was investigated using 3D spheroid-forming HeLa, A549, 293T, SH-SY5Y, and U-2OS cell lines. In addition, adenosine triphosphate (ATP) production and morphological changes of 3D spheroids were monitored in real-time over 7 days.

Materials and methods
Materials
The following cell lines were obtained from NanoEnTek Inc. (Seoul, Korea): prostate (DU145), testis (F9), embryonic fibroblast (NIH-3T3), muscle (C2C12), embryonic kidney (293T), neuroblastoma (SH-SY5Y), adenocarcinomic alveolar basal epithelial cell (A549), cervical cancer (HeLa), HeLa contaminant (HEp2), pituitary epithelial-like cell (GH3), embryonic cell (PA317), and osteosarcoma (U-2OS). Dulbecco's Modified Eagle's Medium (DMEM), Roswell Park Memorial Institute (RPMI) medium, fetal bovine serum (FBS), penicillin-streptomycin, Dulbecco's phosphate-buffered saline (DPBS), and Trypsin-EDTA solution (1X: 0.05% porcine trypsin [1:250], 0.53 mM EDTA, and phenol red in HBSS without Ca^{2+} and Mg^{2+}) were from WelGENE Inc. (Seoul, Korea). For the 2D cell viability assay, 96-well microplates from Thermo Scientific™ Nunc™ (C.165305, Waltham, MA, USA) was used. Corning® 96-well spheroid microplates (C.4520; Corning Inc., Corning, NY, USA) were used for 3D spheroid formation assays. CDDP and DMSO were obtained from Sigma Aldrich Co. (St Louis, MO, USA). Cell counting was performed with an automated fluorescence cell counter (Arthur; NanoEnTek). CellTiter-Glo® reagent for measuring ATP levels was purchased from Promega Corporation (Fitchburg, WI, USA). 3D spheroid cell cultures were monitored using the JuLI Stage real-time cell history recorder (NanoEnTek). 3D cell viability was measured using the Infinite Elisa Reader (Tecan Trading AG., Männedorf, Switzerland).

All cells were commercially available, approval from the ethics committee therefore, was not required.

Cell culture
Cells were cultured in RPMI (U-2OS) or DMEM medium (HeLa, SH-SY5Y, C2C12, GH3, NIH-3T3, DU145, F9, A549, 293T, HEp2, and PA317) supplemented with 10% FBS and penicillin-streptomycin (1% 100 units/mL). Medium was replaced two to three times per week. Cells were washed with DPBS pH 7.0; adherent cells were treated with trypsin (0.05%)–EDTA (0.002%), collected, and centrifuged. Cells were aliquoted and 14 to 20 mL were transferred to 75-mL flasks, after which they were passaged every 2 to 4 days.

Spheroid formation assay
HeLa, SH-SY5Y, C2C12, GH3, NIH-3T3, DU-145, F9, A549, 293T, HEp2, and PA317 cells were plated (200 µL) at 5×10^3 to 3×10^4 cells per well into Corning® 96-well

spheroid microplates. These were centrifuged at 1,000 rpm for 5 minutes, incubated for 72 hours in a CO_2 incubator at 37°C, and then transferred to the JuLI stage to confirm spheroid formation.[19]

3D spheroid antiproliferation screening

U-2OS ($2×10^4$), HeLa ($2×10^3$), SH-SY5Y ($2×10^3$), C2C12 ($1.5×10^4$), NIH-3T3 ($1.5×10^4$), A549 ($2×10^3$), 293T ($2×10^3$), and PA317 ($5×10^3$) cells per well were plated (100 µL) into microplates as mentioned earlier. These were centrifuged at 1,000 rpm for 5 minutes, incubated for 72 hours in a CO_2 incubator at 37°C, and then treated with either 100 µL CDDP (50 mM in DMSO and medium, for a final 20 to 320 µM concentration) or 100 µL DMSO in medium (control, 0 µM). Next, plates were centrifuged at 1,000 rpm for 5 minutes at 37°C and transferred to the JuLI stage in a CO_2 incubator at 37°C for antiproliferation screening. Cells were photographed and viability was measured every 30 minutes over 7 days.[20,21]

3D spheroid antiproliferation assay

U-2OS ($1×10^4$), HeLa ($2×10^3$), SH-SY5Y ($2×10^3$), A549 ($2×10^3$), and 293T ($2×10^3$) cells per well were plated (100 µL) into microplates as mentioned earlier. These were centrifuged at 1,000 rpm for 5 minutes, incubated for 72 hours in a CO_2 incubator at 37°C, and then treated with 100 µL CDDP (50 mM in DMSO and medium). The final concentration was 50 to 250 µM for U-2OS, HeLa, SH-SY5Y, and A549 cells and 20 to 100 µM for 293T cells. Next, plates were centrifuged at 1,000 rpm for 5 minutes at 37°C and transferred to the JuLI stage in a CO_2 incubator at 37°C for the antiproliferation assay. Cells were photographed and viability was measured every 30 minutes over 7 days.

3D cell viability assay

U-2 OS ($1×10^4$), HeLa ($2×10^3$), SH-SY5Y ($2×10^3$), A549 ($2×10^3$), and 293T ($2×10^3$) cells per well were plated (100 µL) into microplates as mentioned earlier. These were centrifuged at 1,000 rpm for 5 minutes, incubated for 72 hours in a CO_2 incubator at 37°C, and treated with either 100 µL CDDP (50 mM in DMSO and medium) or 100 µL DMSO in medium (control, 0 µM). The final concentration of CDDP was 50 to 250 µM for U-2OS, HeLa, SH-SY5Y, and A549 cells; and 20 to 100 µM for 293T cells. Next, plates were centrifuged at 1,000 rpm for 5 minutes at 37°C and experiments were performed in triplicate. After 1, 4, and 7 days, 100 µL medium was removed from each well and replaced with 100 µL luminescence reagent (3D CellTiter-Glo®) following the manufacturer's protocol. Plates were incubated for 30 minutes at room temperature and luminescence was measured.[22,23]

Results and discussion
Spheroid formation assay

The following 12 cell lines, DU145, F9, NIH-3T3, C2C12, 293T, SH-SY5Y, A549, HeLa, HEp2, GH3, PA317, and U-2OS, were screened for their ability to form and maintain 3D spheroids, as shown in Figure 1. Of these, eight cell lines maintained a spheroid shape: NIH-3T3, C2C12, 293T, SH-SY5Y, A549, HeLa, PA317, and U-2OS. DU145 and F9 cell lines revealed irregular 3D spheroid shapes (Figure 1) and, like HEp2, had a doubling time too short for cytotoxicity assays. Consequently, they were not selected.

## 3D spheroid cell antiproliferation screening with CDDP

The eight cell lines selected as mentioned earlier were screened in a 3D spheroid cell antiproliferation assay with CDDP, as shown in Figure 2. Cells were photographed 1, 4 (Figure S1 at day 1 and Figure S2 at day 4), and 7 days (Figure 2) after treatment with CDDP. Accordingly, NIH-3T3 and PA317 cell lines formed 3D spheroids, but no morphological change was observed after CDDP treatment, suggesting that they might be insensitive toward the drug. The C2C12 cell line could not maintain a spheroid shape and appeared insensitive to CDDP. HeLa, A549, 293T, SH-SY5Y, and U-2OS cell lines grew well in the presence of DMSO only and were selected for further studies. These examined the cytotoxic effect of 20, 40, 80, 160, and 320 µM CDDP. U-2OS was also included as a reference cell line.
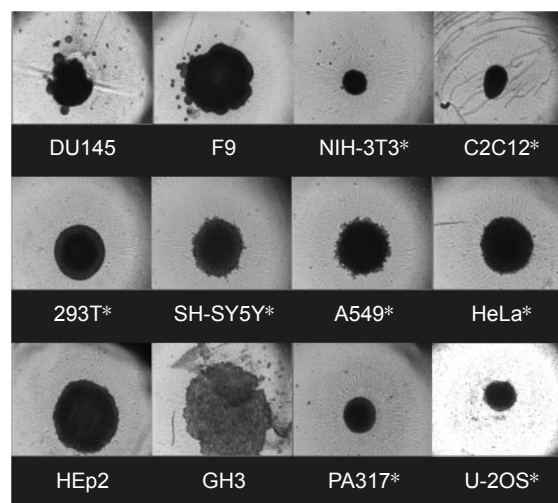
Figure 1 Formation of 3D spheroids after 4 days of culturing.
Notes: 12 cell lines cultured are prostate (DU145), testis (F9), embryo fibroblast (NIH-3T3), muscle cells (C2C12), embryonic kidney cells (293T), neuroblastoma (SH-SY5Y), adenocarcinomic alveolar basal epithelial cell (A549), cervical cancer (HeLa), HeLa contaminant (HEp2), pituitary epithelial-like cells (GH3), another embryo cells (PA317), and osteosarcoma (U-2OS). Selected eight cell lines for further CDDP cytotoxicity study were indicated as *.
Abbreviation: CDDP, cis-diamminedichloridoplatinum (II).
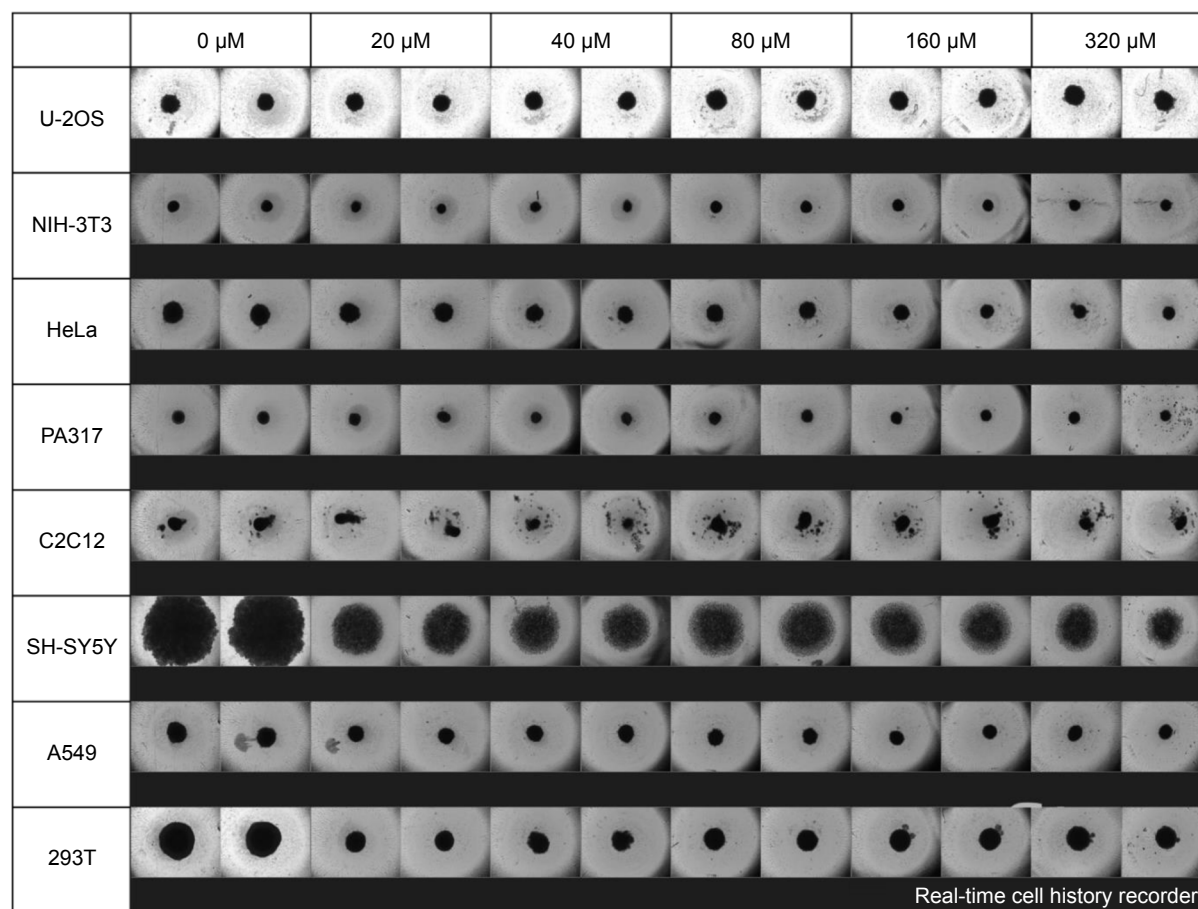
Figure 2 Compiled still shot photos of eight cell lines after 7 days from the treatment with cisplatin.
Note: Cell lines are NIH-3T3, C2C12, 293T, SH-SY5Y, A549, HeLa, PA317, and U-2OS in 96-well plates.

3D spheroid antiproliferation assay with CDDP

The five selected cell lines were treated with 0, 50, and 100 μM CDDP and their diameter was measured every 6 hours, over a total of 158 hours. Morphological results were identical at concentrations of 100 μM or higher as shown in Figure 3 and Table 1. Real-time monitoring of these five cell lines was included in Video S1.

HeLa cells

In the absence of CDDP, HeLa spheroids grew continuously over the entire period, expanding from 350 to 519 μm across. Cells treated with 50 and 100 μM CDDP shrunk slightly between 0 and 12 hours, the diameter of spheroids grew slowly in the first 24 hours after treatment, and stayed constant thereafter. Overall, spheroid diameter increased by 160, 9, and 16 μm following treatment with 0, 50, and 100 μM CDDP, respectively. Real-time monitoring of cell movements and divisions revealed that cells were dying from the periphery of spheroids to the core in a CDDP dose-dependent manner. Spheroid shape

was maintained regardless of CDDP concentration, suggesting that cell binding and/or cross-linking with the extracellular matrix occurred during spheroid formation, thus stabilizing the structure. Cytotoxicity was observed at all CDDP concentrations, but was apparent only after 24 hours, suggesting that it first required endocytosis of CDDP.

A549 cells

In the absence of CDDP, A549 spheroids shrunk slightly from 669 to 528 μm at the end of the experiment. A similar decrease was observed also with 50 μM CDDP, whereby spheroid diameter declined from 646 to 473 μm. At 100 μM CDDP, spheroids shrunk from 597 to 399 μm during the first 40 hours, at which point all cells appeared dead. Overall, the spheroid diameter changed by −141, −173, and −198 μm following treatment with 0, 50, and 100 μM of CDDP, respectively. The diameter was reduced even further at 150 μM CDDP. As with HeLa, real-time monitoring revealed that cells were dying from the periphery of spheroids to the core. Cells treated with 50 μM CDDP stayed active even
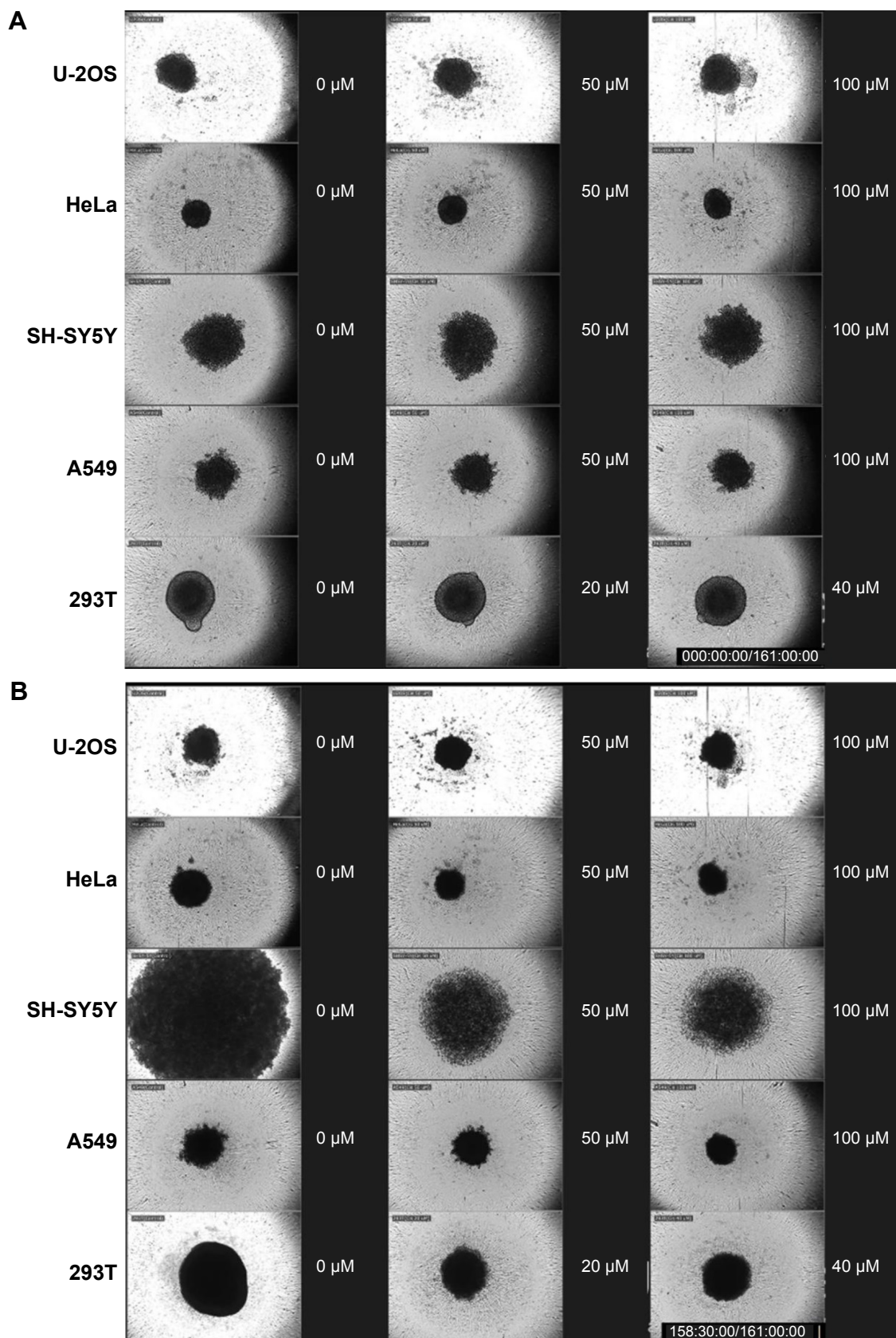
Figure 3 Still shots of five spheroid cell lines after CDDP treatment.
Notes: Spheroids with CDDP at 0, 50, and 100 μM for U-2OS, HeLa, SH-SY5Y, and A549 cell lines, and at 0, 20, and 40 μM for 293T cell line at time 0 (**A**) and at 158 hours (**B**).
Abbreviation: CDDP, cis-diamminedichloridoplatinum (II).

Table 1 Changes in the size of spheroids

Cell line	CDDP (μM)				
	0 (control)	20	40	50	100
HeLa	160	NA	NA	9	19
A549	−141	NA	NA	−173	−198
293T	247	−56	−23	NA	NA
SH-SY5Y	1,250	NA	NA	442	334
U-2OS	−49	NA	NA	−119	−74

Note: Unit of diameters is in μm.
Abbreviations: CDDP, cis-diamminedichloridoplatinum (II); NA, not applicable.

after 156 hours, suggesting that A549 cells could tolerate low doses of CDDP. By contrast, cytotoxicity was immediate at 100 μM CDDP. Finally, as with HeLa, the shape of A549 spheroids was maintained at all CDDP concentrations, confirming the role of the extracellular matrix.

293T cells

In the absence of CDDP, 293T spheroids grew continuously for up to 96 hours, expanding from 613 to 860 μm. The size of spheroids treated with 50 and 100 μM CDDP did not change substantially. Overall, spheroid diameter changed by 247, −56, and −23 μm following treatment with 0, 50, and 100 μm CDDP, respectively. As with A549 cells, CDDP cytotoxicity had an immediate effect. Again, cells appeared to die from the periphery of spheroids to the core, but cellular activity could still be observed at the periphery at all CDDP concentrations. Thus, CDDP could block 293T cell growth, but without killing all cells. This may be explained by the development of drug resistance or the fast metabolism typical of 293T cells. The shape of spheroids was maintained in all treated cells.

SH-SY5Y cells

In the absence of CDDP, SH-SY5Y spheroids grew continuously over the entire period, expanding from 669 to 2,048 μm after 156 hours. Within 36 hours, the diameter of treated spheroids changed by 442 and 334 μm following treatment with 50 and 100 μM CDDP, respectively. Upon closer examination by continuous monitoring, SH-SY5Y spheroids became segregated from each other and failed to maintain their canonical shape, suggesting that CDDP elicited cell death and extracellular matrix dissolution. It is possible that immediate cytotoxicity promoted the release of proteases aimed at degrading the extracellular matrix and segregating dead cells. Up to 96 hours after 50 μM CDDP treatment, minor cellular movements could be detected at the core of spheroids.

U-2OS cells

U-2OS spheroid was used as reference, and its size did not change appreciably with or without CDDP. Overall, the

diameter of spheroids changed by −49, −119, and −74 μm following treatment with 0, 50, and 100 μM CDDP, respectively. Upon closer examination, shape of U-2OS spheroids was maintained, but cellular movements or divisions were blocked both at the periphery and core of spheroids treated with CDDP.

3D spheroid cell antiproliferation assay

The tumor microenvironment has been implicated in tumor growth, metastasis, and resistance to anticancer therapies. The influence of the microenvironment on the growth pattern of each cell line in the absence of CDDP was monitored in real-time (Video S1). Initially, 293T, HeLa, and U-2OS spheroids exhibited a distinct periphery, an intermediate part, and a core. In 293T, proliferating cells were concentrated at the periphery. Cellular activities in HeLa and U-2OS were found at the periphery and intermediate regions. For A549 and SH-SY5Y spheroids, no distinction between periphery and intermediate regions could be made, and proliferation occurred across SH-SY5Y spheroids. U-2OS and 293T spheroids at 0 μM maintained a distinction between regions over the course of the experiment, whereas the HeLa spheroid at 0 μM exhibited increased cell proliferation in the core and reduced proliferation in the intermediate region. CDDP generally resulted in a denser spheroid core, loss of proliferation in the intermediate region, and a drop in measurable peripheral movement. Instead, in SH-SY5Y spheroids, CDDP induced a rapid expansion followed by core collapse. The effect over time of CDDP on the spheroid core, intermediate regions, and periphery is shown in Table 2.

Table 2 Observable effects of CDDP on multiple spheroidal cell lines over 24 hours

Cell line	Spheroid			
Concentration of CDDP	Periphery	Intermediate	Core	Expansion/motion
293T				
0 μM	Yes	Yes	Yes	Yes/Yes
60 μM	No	No	No	No/Yes
A549				
0 μM	Yes	No	Yes	Yes/Yes
150 μM	No	No	No	No/No
HeLa				
0 μM	Yes	No	Yes	Yes/Yes
150 μM	No	No	No	No/No
SH-SY5Y				
0 μM	Yes	Yes	Yes	Yes/Yes
150 μM	No	No	No	No/No
U-2OS				
0 μM	Yes	Yes	Yes	Yes/Yes
150 μM	No	No	No	No/No

Abbreviation: CDDP, cis-diamminedichloridoplatinum (II).

3D cell viability assay: ATP, comparison with the antiproliferation assay

Figure 4 shows changes in ATP activity of U-2OS, HeLa, SH-SY5Y, A549, and 293T spheroids incubated with increasing concentrations of CDDP for 1, 4, and 7 days. Their IC_{50} values are listed in Table 3. During the first day, U-2OS, A549, and 293T spheroids revealed sigmoidal responses to increasing CDDP concentrations; whereas, HeLa and SH-SY5Y spheroids were more sensitive to CDDP and exhibited

exponential responses. This observation advocated the use of lower CDDP doses in future experiments. On day 4, ATP activity of U-2OS, HeLa, and SH-SY5Y cells collapsed; whereas, A549 and 293T spheroids retained significant ATP activity. A549 and 293T spheroids exhibited similar ATP activity even on day 7. Based on IC_{50} data and total spheroid ATP activity (days 1, 4, and 7), sensitivity to CDDP was lowest in A549, followed by 293T, HeLa, U-2OS, and SH-SY5Y cells. The activity profile of 293T spheroids on days
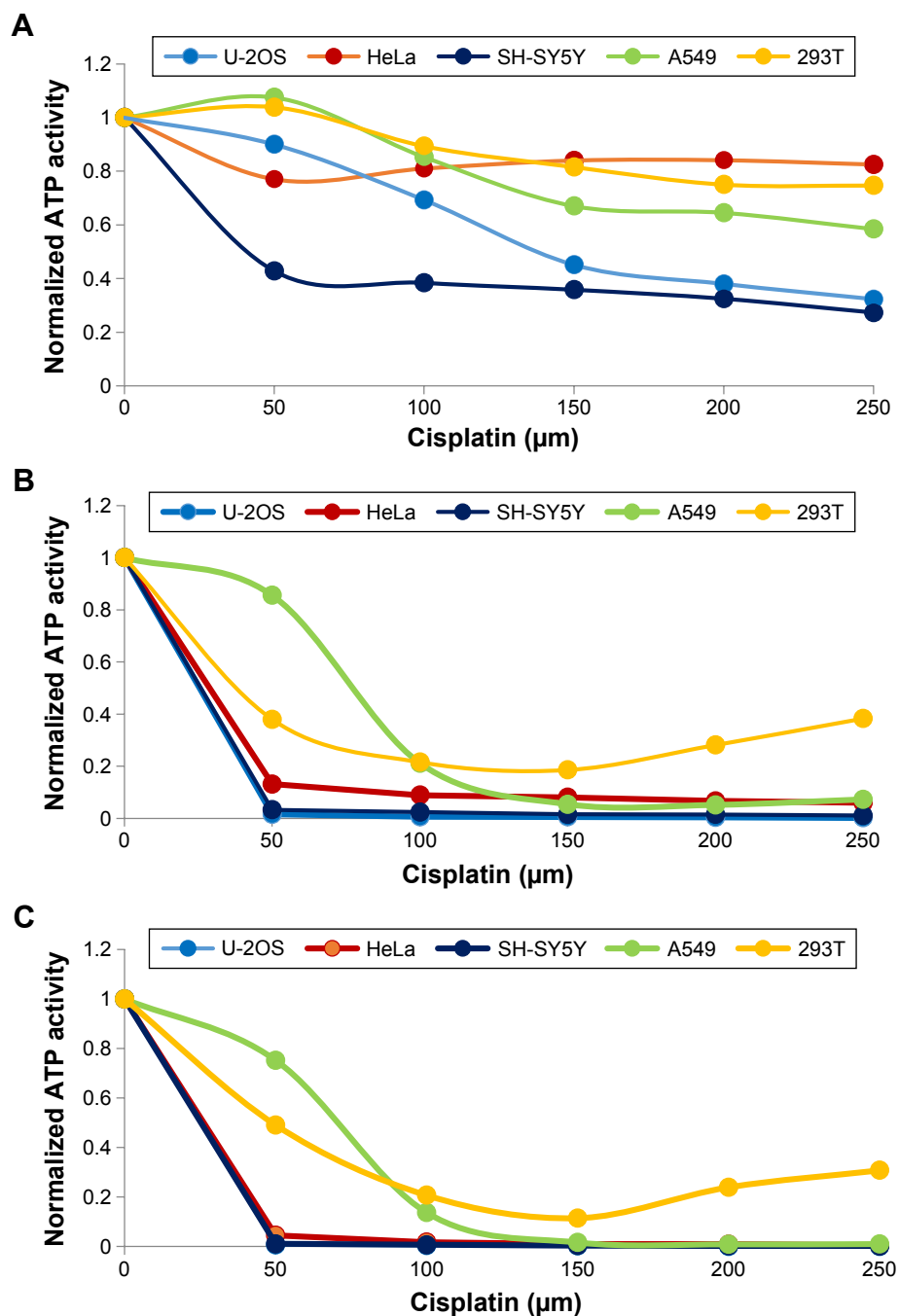
Figure 4 The effect of increasing cisplatin concentrations on U-2OS, HeLa, SH-SY5Y, A549, and 293T spheroidal ATP activity after (**A**) 1 day, (**B**) 4 days, and (**C**) 7 days of incubation.
Abbreviation: ATP, adenosine triphosphate.

Table 3 Effect of incubation times on the CDDP IC_{50} values of A549, 293T, HeLa, U-2OS, and SH-SY5Y spheroids in comparison with results from previously reported 2D experiments

	Day	A549	293T	HeLa	U-2OS	SH-SY5Y
3D	1	>250	>250	>250	122	23.5
	4	80.7	19	21.5	17.4	16.5
	7	78.6	33	21.4	18.3	15.6
2D		64[29]	14[30]	9.4[31]	5.6[32]	8.5[33]

Note: Unit of IC_{50} is in µM.
Abbreviations: CDDP, cis-diamminedichloridoplatinum (II); 2D, two-dimensional; 3D, three-dimensional.

4 and 7 suggested a pattern of CDDP resistance. Whether this occurred spontaneously or not, chronic resistance was previously unknown in this cell line and may warrant further testing.

Comparison of 2D and 3D cultures

According to a study by Wang et al, IC_{50} values of CDDP against ES-2, SKOV-3, and OVCAR-3 cells in 2D cultures were 8.975, 37.111, and 11.741 µM, respectively.[9] Another study reported that IC_{50} values of CDDP against 2D Hep3B and HepJ5 cultures were 5.38 and 2.37 µM, respectively.[15] IC_{50} values of CDDP against Saos-2 in 2D and 3D cultures were 0.12 and 0.3 µM, respectively.[19] Similarly, IC_{50} values of CDDP against HOS in 2D and 3D cultures were 0.12 and 2.5 µM, respectively.[18] Hence, higher cytotoxicity was observed in 2D than in 3D settings.[21] Here, IC_{50} values of CDDP against U-2OS, HeLa, SH-SY5Y, 293T, and A549 spheroids were compared with results from the 2D system by previously reported values, as listed in Table 3. IC_{50} values for all spheroids were higher than results from the 2D system, supporting higher cytotoxicity in 2D than in 3D system. The results would not be a direct comparative representation between 2D and 3D system, since the IC_{50} values were taken at day 2 for 2D system and day 4 for 3D system. But the much higher IC_{50} values for spheroids could be approximated by using results from day 1 and day 4. Overall, higher concentrations of CDDP would be required to observe the cytotoxicity in 3D spheroids than in 2D system.

CDDP treatment has been associated with metabolic alterations and DNA damage, disturbing signaling and cell proliferation pathways. Affected genes include *p53*, *MAP-kinases ERK1/2*, and *Akt1*.[24–26] The 24-hour delay in the appearances of an initial cytotoxic response could depend on endocytosis and intracellular trafficking being required for toxicity. The extracellular matrix seems essential in maintaining intact 3D spheroids. Hence, the gradient of cell death from the periphery to the core would depend on both diffusion and 3D structure. However, ATP generation was blocked immediately, suggesting that effectiveness of CDDP was also

immediate. Because cells were not labeled with fluorescent tags or other markers, reactive oxygen species generation, cytokine release, or oxygen consumption were not measured in the current study. In a previous report by Alborzinia et al, oxygen consumption was shown to be one of the earliest parameters affected by CDDP,[27] suggesting a strong link between CDDP cytotoxicity and mitochondria. Such link is supported by the current drastic decrease in ATP generation. Interestingly, CDDP-mediated DNA damage was noticed in HEK293T cells,[28] indicating that CDDP may accumulate and bind to mitochondrial DNA, thus damaging these organelles. Our results are in good agreement with previous reports of DNA damage as the main mode of CDDP function.

ATP measurements reflected changes in cell morphology and movement, typical of cell–cell and cell–extracellular matrix interactions. Except for 293T, all cell lines treated with CDDP (at any concentration) showed a rapid loss of ATP generation after 1 day. 293T spheroids exhibited lower, yet sustained, ATP generation, indicating the existence of resistant 293T or fast metabolic clearance of CDDP due to a higher glycolytic flux in these cells.

Conclusion

Five human cell lines, HeLa, A549, 293T, SH-SY5Y, and U-2OS, were selected. Based on their ability to form and maintain 3D spheroids, real-time cytotoxicity of CDDP, one of the best-studied anticancer agents, was assessed. Morphological changes and ATP generation of 3D spheroids were recorded and measured. Following CDDP treatment, cell growth of 3D spheroids and ATP generation by the corresponding cells stopped over time in a dose-dependent manner. The ability to form and maintain a 3D spheroid shape could be determined by cell–cell communication, cell networks, and interactions mediated by binding or cross-linking of surface proteins, receptors, and ligands. Cells killed by CDDP would maintain the spheroid shape and round structure thanks to the extracellular matrix. The benefit of 3D spheroids lies in their model representation of tumors. Along with wound healing and transfection efficiency, the cytotoxic mechanisms of anticancer agents would be better understood if accompanied by real-time 3D cell culture and other proliferation and apoptosis assays. The maintenance of stable experimental conditions for long periods will be crucial for the continuous monitoring in drug testing experiments.
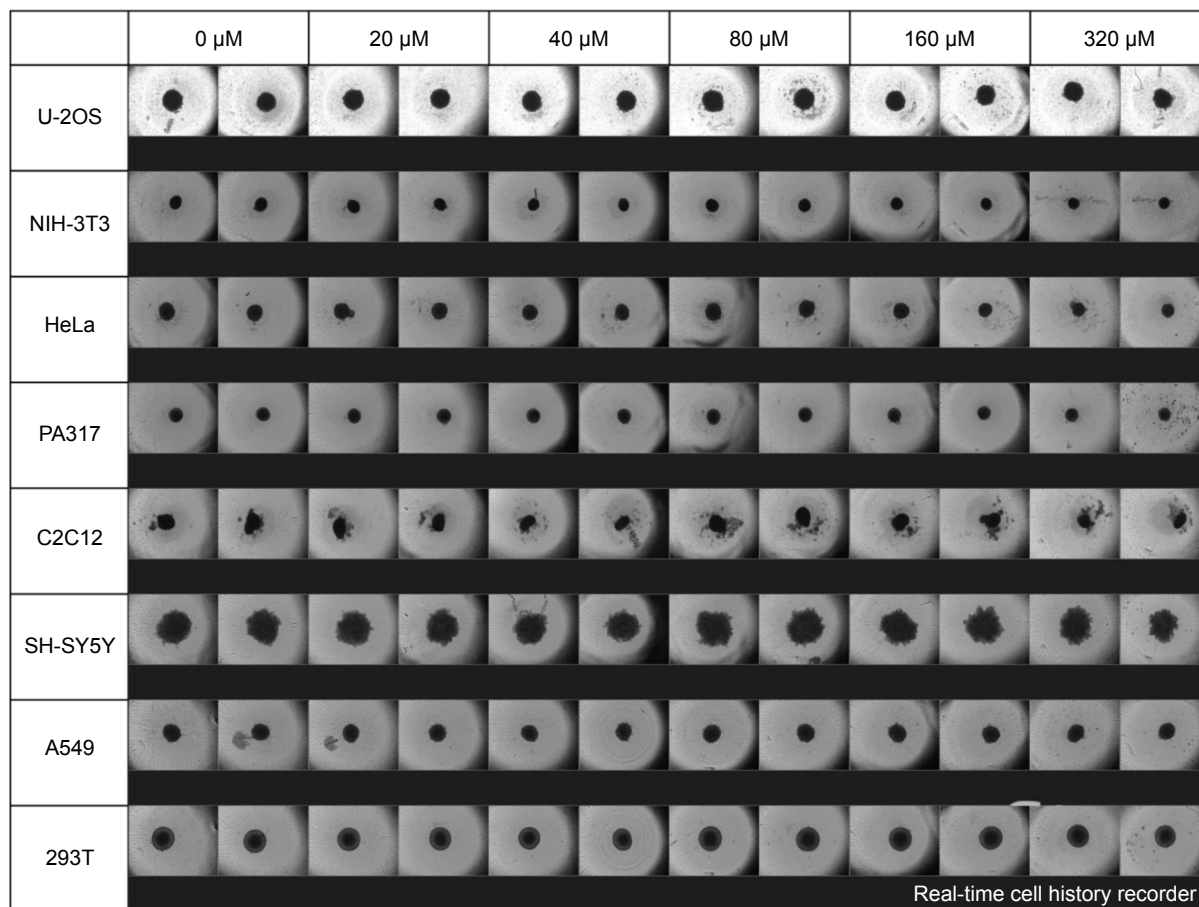
Acknowledgment

Disclosure

The authors report no conflict of interest in this work.

References

1. Howard D, Buttery LD, Shakesheff KM, Roberts SJ. Tissue engineering: strategies, stem cells and scaffolds. *J Anat*. 2008;213(1):66–72.
2. Ravi M, Paramesh V, Kaviya SR, Anuradha E, Solomon FD. Review. 3D cell culture systems: advantage and applications. *J Cell Physiol*. 2015;230(1):16–26.
3. Pampaloni F, Reynaud EG, Stelzer EH. The third dimension bridges the gap between cell culture and live tissue. *Nat Rev Mol Cell Biol*. 2007; 8(10):839–845.
4. Folberg R, Arbieva Z, Moses J, et al. Tumor cell plasticity in uveal melanoma: microenvironment directed dampening of the invasive and metastatic genotype and phenotype accompanies the generation of vasculogenic mimicry patterns. *Am J Pathol*. 2006;169(4):1376–1389.
5. Mikhail AS, Eetezadi S, Allen C. Multicellular tumor spheroids for evaluation of cytotoxicity and tumor growth inhibitory effects of nanomedicines *in vitro*: a comparison of docetaxel-loaded block copolymer micelles and taxotere. *PLoS One*. 2013;8(4):e62630.
6. Dolznig H, Rupp C, Puri C, et al. Modeling colon adenocarcinomas *in vitro*: a 3D co-culture system induces cancer-relevant pathways upon tumor cell and stromal fibroblast interaction. *Am J Pathol*. 2011; 179(1):487–501.
7. Vinci M, Gowan S, Boxall F, et al. Advances in establishment and analysis of three-dimensional tumor spheroid-based functional assays for target validation and drug evaluation. *BMC Biol*. 2012;10:29.
8. Lee JM, Mhawech-Fauceglia P, Lee N, et al. A three-dimensional microenvironment alters protein expression and chemosensitivity of epithelial ovarian cancer cells *in vitro*. *Lab Invest*. 2013;93(5):528–542.
9. Wang CW, Chen CL, Wang CK, et al. CDDP-, doxorubicin-, and docetaxel-induced cell death promoted by the aqueous extract of solanum nigrum in human ovarian carcinoma cells. *Integr Cancer Ther*. 2015; 14(6):546–555.
10. Baik MH, Friesner RA, Lippard SJ. Theoretical study of CDDP binding to purine bases: why does CDDP prefer guanine over adenine? *J Am Chem Soc*. 2003;125(46):14082–14092.
11. Ni P, Xu W, Zhang Y, et al. TXNL1 induces apoptosis in CDDP resistant human gastric cancer cell lines. *Curr Cancer Drug Targets*. 2015; 14(9):850–859.
12. Kim DW, Kim KO, Shin MJ, et al. siRNA-based targeting of antiapoptotic genes can reverse chemoresistance in P-glycoprotein expressing chondrosarcoma cells. *Mol Cancer*. 2009;8:28.
13. Köppen C, Reifschneider O, Castanheira I, Sperling M, Karst U, Ciarimboli G. Quantitative imaging of platinum based on laser ablation-inductively coupled plasma-mass spectrometry to investigate toxic side effects of CDDP. *Metallomics*. 2015;7(12):1595–1603.
14. Lin LT, Tai CJ, Su CH, et al. The ethanolic of *Taiwanofungus camphoratus* (*Antrodia camphorata*) induces cell cycle arrest and enhances cytotoxicity of CDDP and doxorubicin on human hepatocellular carcinoma cells. *Biomed Res Int*. 2015;2015:415269.
15. Flores-Pérez A, Rafaelli LE, Ramírez-Torres N, et al. RAD50 targeting impairs DNA damage response and sensitizes human breast cancer cells to CDDP therapy. *Cancer Biol Ther*. 2014;15(6):777–788.
16. Gambari R, Hau DK, Wong WY, Chui CH. Sensitization of Hep3B hepatoma cells to CDDP and doxorubicin by corilagin. *Phytother Res*. 2014;28(5):781–783.
17. Chitcholtan K, Sykes PH, Evans JJ. The resistance of intracellular mediators to doxorubicin and CDDP are distinct in 3D and 2D endometrial cancer. *J Transl Med*. 2012;10:38.
18. Gibot L, Wasungu L, Teissié J, Rols MP. Antitumor drug in multicellular spheroids by electropermeabilization. *J Control Release*. 2013; 167(2):138–147.
19. Rimann M, Laternser S, Gvozdenovic A, et al. An *in vitro* osteosarcoma 3D microtissue model for drug development. *J Biotechnol*. 2014;189:129–135.
20. Mandal BB, Kundu SC. Cell proliferation and migration in silk fibroin 3D scaffolds. *Biomaterials*. 2009;30(15):2956–2965.
21. Ng KW, Leong DTW, Hutmacher DW. The challenge to measure cell proliferation in two and three dimensions. *Tissue Eng*. 2005; 11(1–2):182–191.
22. Al Shammari B, Shiomi T, Tezera L, et al. The extracellular matrix regulates granuloma necrosis in tuberculosis. *J Infect Diseases*. 2015; 212(3):463–473.
23. Auld DS, Zhang YQ, Southall NT, et al. A basis for reduced chemical library inhibition of firefly luciferase obtained from directed evolution. *J Med Chem*. 2009;52(5):1450–1458.
24. Kim HS, Hwang JT, Yun H, et al. Inhibition of AMP-activated protein kinase sensitizes cancer cells to cisplatin-induced apoptosis via hyper-induction of p53. *J Biol Chem*. 2008;283(7):3731–3742.
25. Datta SR, Brunet A, Greenberg ME. Cellular survival: a play in three Akts. *Genes Dev*. 1999;13(22):2905–2927.
26. Panka DJ, Cho DC, Atkins MB, Mier JW. GSK-3beta inhibition enhances sorafenib-induced apoptosis in melanoma cell lines. *J Biol Chem*. 2008;283(2):726–732.
27. Alborzinia H, Can S, Holenya P, et al. Real-time monitoring of cisplatin-induced cell death. *PLoS One*. 2011;6(5):e19714.
28. Tompkins JD, Wu X, Her C. MutS homologue hMSH5: role in cisplatin-induced DNA damage response. *Mol Cancer*. 2012;11:10.
29. Zhang P, Gao WY, Turner S, Ducatman BS. Gleevec (STI-571) inhibits lung cancer cell growth (A549) and potentiates the cisplatin effect in vitro. *Mol Cancer*. 2003;2:1.
30. Sohn SH, Ko E, Jo Y, et al. The genome-wide expression profile of *Paeonia suffruticosa*-treated cisplatin-stimulated HEK 293 cells. *Environ Toxicol Pharmacol*. 2009;28(3):453–458.
31. Putral LN, Bywater MJ, Gu W, et al. RNA interference against human papillomavirus oncogenes in cervical cancer cells results in increased sensitivity to cisplatin. *Mol Pharmacol*. 2005;68(5):1311–1319.
32. Graat HCA, Witlox MA, Schagen FHE, et al. Different susceptibility of osteosarcoma cell lines and primary cells to treatment with oncolytic adenovirus and doxorubicin or cisplatin. *Br J Cancer*. 2006; 94(12):1837–1844.
33. Hussein D, Holt SV, Brookes KE, et al. Preclinical efficacy of the bioreductive alkylating agent RH1 against paediatric tumours. *Br J Cancer*. 2009;101(1):55–63.

Supplementary materials

	0 µM	20 µM	40 µM	80 µM	160 µM	320 µM
U-2OS						
NIH-3T3						
HeLa						
PA317						
C2C12						
SH-SY5Y						
A549						
293T						

Real-time cell history recorder

Figure S1 Still shots of eight spheroid cell lines at 1 day after CDDP treatment.
Abbreviation: CDDP, Cis-diamminedichloridoplatinum (II).
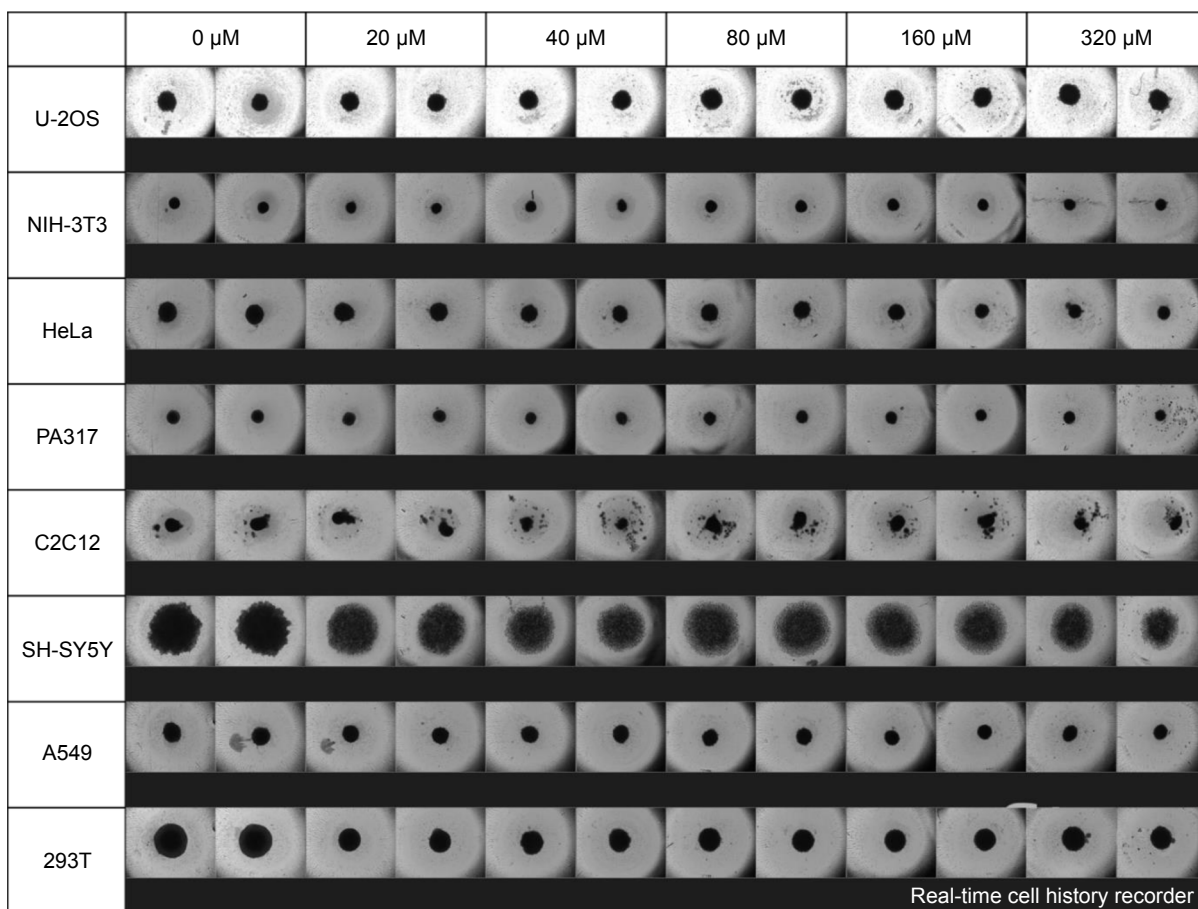
Figure S2 Still shots of eight spheroid cell lines at 4 days after CDDP treatment.
Abbreviation: CDDP, Cis-diamminedichloridoplatinum (II).